Applied Catalysis B: Environmental 196 (2016) 135–141

Contents lists available at ScienceDirect

Applied Catalysis B: Environmental

journal homepage: www.elsevier.com/locate/apcatb

A surface science approach to TiO_2 P25 photocatalysis: An *in situ* FTIR study of phenol photodegradation at controlled water coverages from sub-monolayer to multilayer

Lorenzo Mino [a,*], Adriano Zecchina [b], Gianmario Martra [b], Andrea Mario Rossi [a], Giuseppe Spoto [b]

[a] National Institute of Metrological Research (INRIM), Strada delle Cacce 91, Torino, Italy
[b] Department of Chemistry and NIS Centre, University of Torino, via Giuria 7, Torino, Italy

ARTICLE INFO

Article history:
Received 16 February 2016
Received in revised form 9 May 2016
Accepted 16 May 2016
Available online 17 May 2016

Keywords:
Phenol photodegradation
TiO_2 P25
Adsorbed water
FTIR spectroscopy
Degradation kinetics

ABSTRACT

The photodegradation of phenol on TiO_2 P25 has been investigated by a transmission FTIR set-up allowing to monitor the processes occurring at the oxide surface during photocatalytic reactions under *in situ* UV–vis irradiation and in controlled atmosphere, after sending well-defined doses of adsorbates. This approach helps to close the gap between conventional surface science studies and investigations carried out in solution. The study of the mechanism of adsorption demonstrates that phenol dosed from the gas phase on the dehydroxylated surface readily dissociates to form OH groups and adsorbed phenolate species. After completion of the monolayer, further phenol is adsorbed in molecular form to build a multilayer. The state of adsorbed phenol in presence of increasing amounts of co-adsorbed water has also been accurately monitored. During UV–vis irradiation the main phenol signals progressively decrease, while new bands appear, ascribed to the formation of adsorbed oxalates and carbonates. Also the presence of small quantities of catechol and hydroquinone cannot be excluded. The pseudo-first order rate constant for the phenol photodegradation results to be strongly dependent on the surface hydration conditions and increases of one order of magnitude moving from a nearly dehydrated surface to a surface with a multilayer of liquid-like adsorbed water *(i.e.* a condition more representative of the processes occurring at the oxide surface when TiO_2 is immersed in solution like in most applications).

1. Introduction

Photoinduced chemical reactions over TiO_2 play an essential role in many applications including self- cleaning of TiO_2-containing substrates and photodegradation of a large number of pollutants. The importance of this research field is testified by the exponential growth of publications on TiO_2 photocatalysis that appeared in the last two decades [1–3].

As underlined by Serpone et al. [4], this explosive growth of interest in the practical applications of nanosized TiO_2 was not accompanied by a parallel growth of fundamental studies concerning the spectroscopy of trapped photoelectrons and holes and of surface species generated at specific surface sites upon irradiation, although some insights have been obtained using time resolved MIR absorption spectroscopy which can effectively monitor the kinetics of photogenerated electrons [5,6].

These issues are particularly relevant when the surface properties under irradiation of water immersed TiO_2 interfaces are considered, which are playing a key role in the cleaning of wastewaters in presence of oxygen. In this regard, few attenuated total reflectance Fourier transform infrared spectroscopy (ATR-FTIR) investigations tried to follow the evolution of the oxide surface during the photodegradation of organic pollutants, like oxalic acid [7–10], malonic acid [8], succinic acid [8], carbofuran [11] and catechol [7]. However, the ATR acquisition mode suffers some limitations in terms of sensitivity, quantification and spectral quality with respect to transmission FTIR spectroscopy and the employed experimental set-ups often do not ensure a full control of the experimental conditions. To try to overcome issues, we developed a set-up, exploiting a high transmission, large core liquid light guide, allowing to irradiate *in situ* the oxide sample with an intense UV–vis

* Corresponding author at: Department of Physics, University of Torino, via Giuria 1, Torino, Italy.
E-mail address: lorenzo.mino@unito.it (L. Mino).

http://dx.doi.org/10.1016/j.apcatb.2016.05.029
0926-3373/

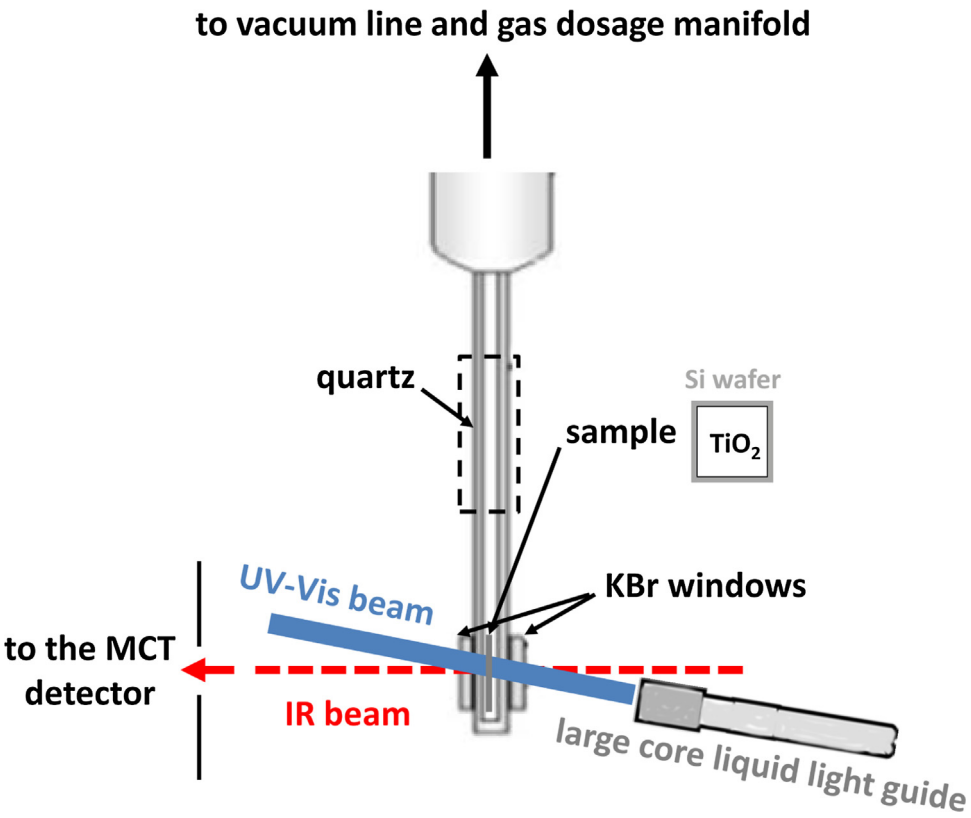

Fig. 1. a) Scheme of the experimental set-up showing the paths of the IR and UV–vis beams which are focused on the TiO_2 sample placed in controlled atmosphere inside a homemade quartz cell equipped with KBr optical windows. The dashed black box highlights the part of the IR cell used to perform the thermal treatments on the sample by means of an external furnace.

beam while acquiring transmission FTIR spectra in controlled atmosphere (see Section 2 for further details). This set-up was employed to study the photodegradation of phenol adsorbed on the clean surface of TiO_2 P25 in presence of variable coverages of co-adsorbed water. Indeed, by dosing water from the gas phase, it is possible to vary the adsorbed water coverage in a controlled way from fractions of a monolayer to few layers, using pressures near to the equilibrium vapor pressure [12].

Phenol is one of the most important water organic pollutants and its photodegradation mechanism has been intensively studied [13,14]. The methods usually adopted monitor the evolution with illumination time of the concentration of photodegradation products present in the solution where TiO_2 is immersed. However the investigation of the structure of the species (adsorbed phenol and degradation products) present on the oxide surface under illumination in controlled atmosphere would be crucial to further clarify the degradation mechanism. Therefore, in this paper we present a time resolved transmission FTIR study of the reactivity under *in situ* UV–vis illumination of phenol adsorbed in controlled atmosphere on the TiO_2 P25 surface in presence of different well-defined amounts of water (from sub-monolayer to multilayer conditions).

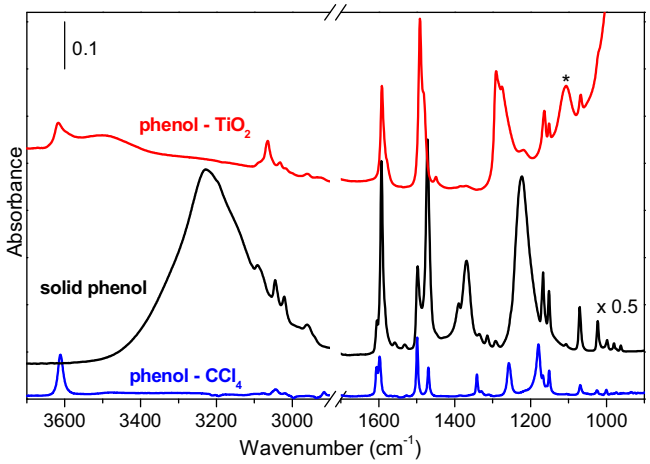

Fig. 2. Comparison of FTIR ATR spectrum of solid phenol (black curve) and FTIR transmission spectra of a diluted phenol solution in CCl_4 (blue curve) and of phenol adsorbed on activated TiO_2 P25 (red curve) deposited on a Si wafer. The asterisk highlights a band arising from the Si-O vibration due to oxygen impurities in the Si wafer used as a support for the TiO_2 P25 film (see Section 2). (For interpretation of the references to color in this figure legend, the reader is referred to the web version of this article.)

2. Experimental

TiO_2 used in these experiments was commercial Evonik (formerly Degussa) P25, which is considered a benchmark in the field of photocatalysis. P25 is prepared by flame hydrolysis of $TiCl_4$ and contains a mixture of about 85% anatase and 15% rutile with a surface area of about 60 m^2/g [15,16]. For the IR measurements under *in situ* UV–vis irradiation P25 was deposited on IR transparent Si wafers by doctor blade method to obtain thin films of suitable thickness to ensure that the entire sample thickness sampled by the IR beam is also reached by the UV–vis radiation.

Before adsorbing phenol from the gas phase, the TiO_2 samples were outgassed in a homemade quartz cell equipped with KBr optical windows (see Fig. 1) at 773 K for 2 h under high vacuum (residual pressure < 10^{-4} mbar), then oxidized with 15 mbar O_2 and cooled down to 293 K in O_2 atmosphere. The treatment with O_2 was performed to ensure the full stoichiometry of the oxide, which will be

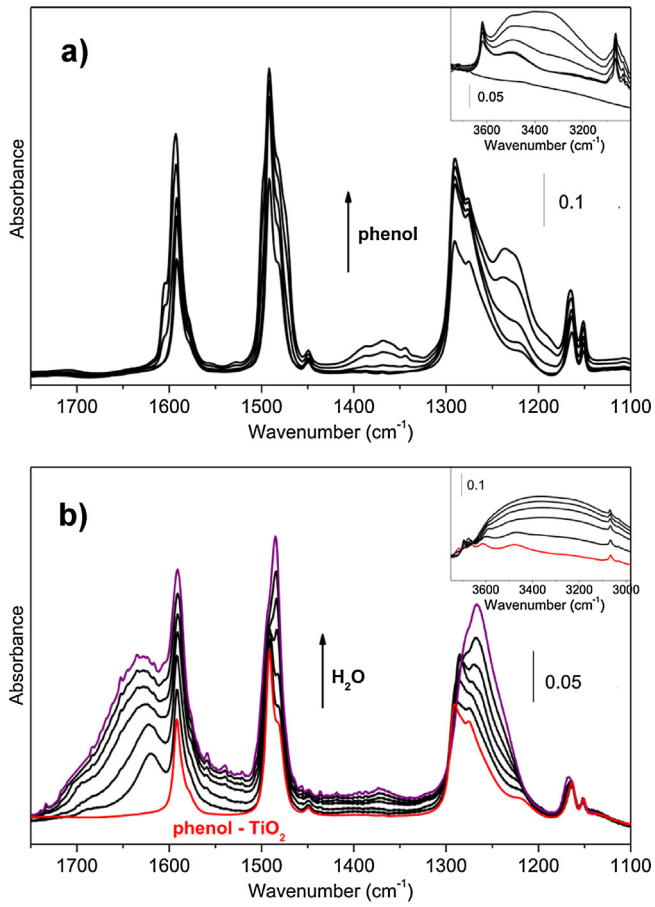

Fig. 3. a) FTIR spectra of phenol adsorbed via vapour phase at progressively increasing coverages on TiO_2 P25 previously outgassed at 773 K. The spectrum of the activated material has been subtracted from all spectra. In the inset the OH and CH stretching modes spectral region is reported. b) As part a) showing the effect of increasing water pressures (0.1, 0.5, 1, 3, 6 and 10 mbar of H_2O, black spectra) on pre-adsorbed phenol (red spectrum).

named activated P25 in the following. Phenol and water were dosed from the gas phase by means of a vacuum manifold permanently attached to the IR cell.

The infrared spectra were recorded on a Bruker IFS 28 FTIR spectrometer, equipped with an MCT cryogenic detector; 64 interferograms (recorded at 2 cm^{-1} resolution) were typically averaged for each spectrum. The Attenuated Total Reflectance (ATR) spectrum of solid phenol was recorded by means of a Specac's Golden Gate single reflection diamond ATR accessory

In situ photodegradation experiments were performed using a Newport 500 W Hg(Xe) arc lamp, equipped with a water filter to eliminate the infrared portion of the spectrum. The radiation emitted by the lamp was focused on the TiO_2 sample using an aspherical fiber bundle focusing assembly and a large core (3 mm) Newport liquid light guide. The measured irradiance at the sample position was 70 W/m^2 in the 315–400 nm range and 240 W/m^2 in the 400–1050 nm range; the complete spectral irradiance curve at the sample position is reported in Fig. S1 in the supplementary data.

This set-up (Fig. 1) allowed to irradiate the TiO_2 sample inside the quartz cell in controlled atmosphere with an intense UV–vis beam with a spot size comparable to the IR beam (*ca.* 5 mm diamater). A similar UV-light guide has been recently exploited to study the photooxidation of methanol using an in flow *operando* set-up [17,18].

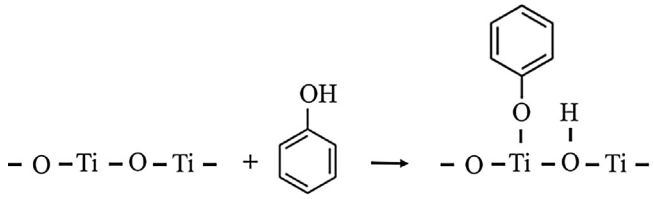

Scheme 1. Reaction between the activated TiO_2 surface and the phenol molecule, which leads to the formation of an OH group and an adsorbed phenolate.

3. Results and discussion

3.1. Mechanism of phenol adsorption on TiO_2

The Attenuated Total Reflectance (ATR) spectrum of solid phenol is compared in Fig. 2 with the transmission spectra of a diluted solution of phenol in CCl_4 and of phenol adsorbed on highly dehydroxylated TiO_2. On the basis of previous literature data [19–21], we can immediately recognize in the spectra some features which are important for the following discussion:

- the broad band centered at 3226 cm^{-1} and tailed on the low frequency side of the solid phase (black curve) which is due to the ν(OH) stretching mode of the hydrogen bonded O—H groups; the same vibration for the free OH groups gives rise to a narrow band at 3612 cm^{-1} in diluted CCl_4 solutions and to a broader component at 3617 cm^{-1} when adsorbed on dehydroxylated TiO_2, arising from the dissociative chemisorption of phenol on the clean surface (*vide infra*);
- the weak absorptions due to the ν(CH) stretching vibrations in the 3100–3000 cm^{-1} region, located at 3076, 3044, and 3021 cm^{-1} for diluted phenol solutions in CCl_4, which shift to 3064, 3032 and 3016 cm^{-1} when adsorbed on dehydroxylated TiO_2;
- the ring stretching modes in the 1650–1450 cm^{-1} interval (centered at 1605, 1597, 1498 and 1469 cm^{-1} in CCl_4 solution);
- the manifestation of the δ(OH) mode of phenol consisting in a broad band centered at 1368 cm^{-1} in the solid and in a much narrower absorption at 1342 cm^{-1} in solution; this feature is nearly absent in phenol adsorbed on TiO_2 at low concentrations; this vibration is usually considered as slightly coupled with the ν(CO) stretching giving rise also to the band at 1180 cm^{-1};
- the band due to the ν(CO) vibration at 1223 cm^{-1} in the solid (broad) and at 1256 cm^{-1} in CCl_4 solution (narrow);
- the β(CH) in-plane bending modes centered at 1166 and 1151 cm^{-1} in CCl_4 solution.

A final short comment to Fig. 2 is deserved by the sequence of regularly spaced weak bands observed in the spectrum of solid phenol in the 3000–2300 cm^{-1} interval. This sequence is due to multiple Fermi resonance coupling involving the ν(OH) modes of the hydrogen bonded OH species and combinations or overtones of low frequency vibrations. This coupling is here at the origin of the appearance of a quite regular series of the so called Evans windows [22].

A more detailed analysis of the phenol interaction with TiO_2 surfaces can be performed considering the FTIR spectra of increasing doses of phenol adsorbed from the gas phase on a highly dehydroxylated TiO_2 P25 sample (Fig. 3a). At low phenol coverage the spectra show the main bands at 3617, 3490, 3064, 3032, 3016, 1590, 1490, 1480, 1289, 1273, 1163 and 1151 cm^{-1}. Comparing these spectra with those of pure phenol in the solid state and in solution (Fig. 2), it is immediately evident that the interaction with the surface causes the disappearance of the bands due to the δ(OH) bending in the 1400–1300 cm^{-1} interval as well as of that due the ν(CO) mode in the 1260–1200 cm^{-1} region, the latter being actu-

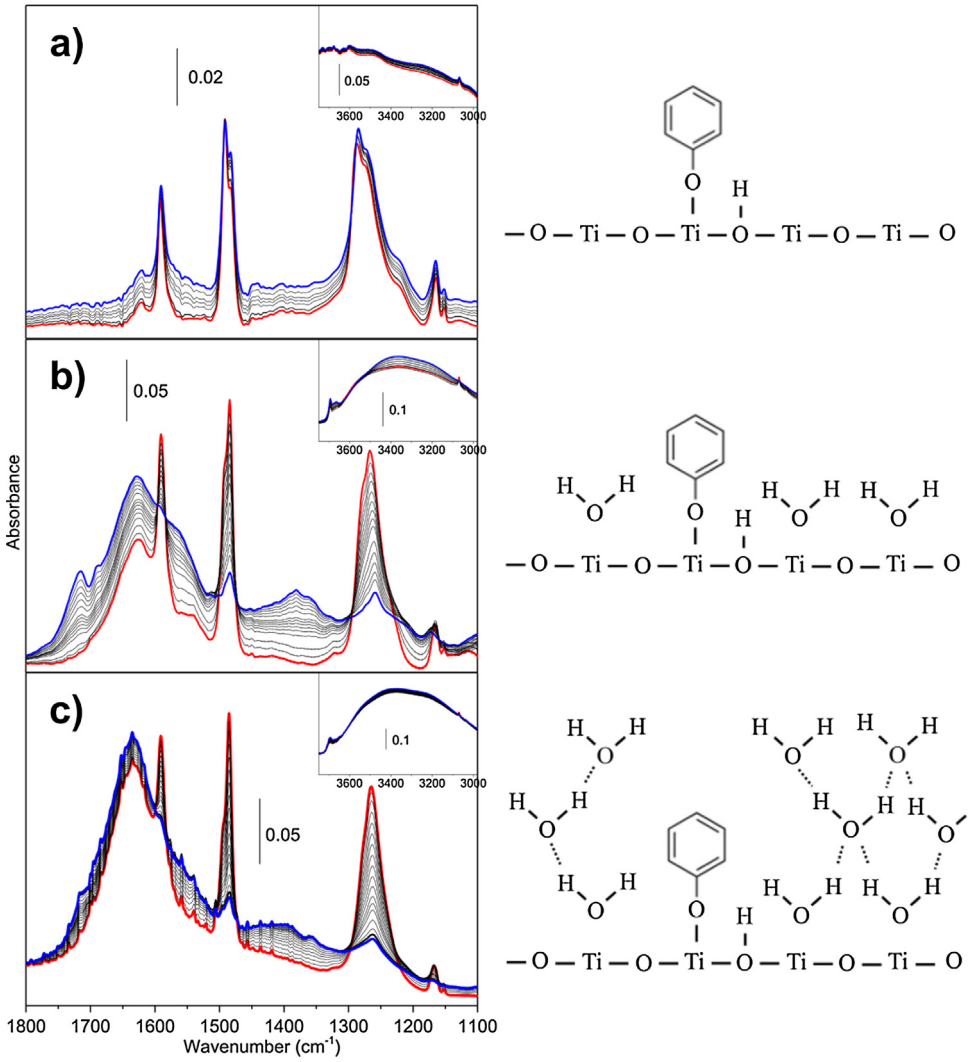

Fig. 4. Photodegradation of phenol adsorbed on activated P25 in presence of 500 mbar of a 20% O_2–80% N_2 mixture and of different amounts of co-adsorbed water: a) traces of molecular water (spectra up to 220 min of UV–vis irradiation); b) surface water monolayer (spectra up to 320 min of UV–vis irradiation); c) 10 mbar of H_2O in equilibrium in the gas phase (spectra up to 210 min of UV–vis irradiation). The spectrum of the activated material has been subtracted from all spectra. In the inset the OH and CH stretching modes spectral region is reported. In the right part a heuristic representation of the different surface hydration conditions for the three spectra is reported.

ally substituted in the adsorbed state by a doublet of absorptions at 1289 and 1273 cm^{-1}. Based also on literature data about phenate anions and neutral phenol species in solution [20], this behavior can be interpreted as the consequence of a reaction between the slightly acidic phenol molecule and the surface –Ti-O- acid-base pairs to form an OH group and a Ti-phenolate, as represented in Scheme 1.

The IR spectrum is substantially different from that expected for a pure phenolate anion, which should show a prominent ν(C=O) band in the 1700–1600 cm^{-1} range [23]. The actual frequency of the ν(CO) mode, that is downward shifted of about 400 cm^{-1}, is indicative of a strong interaction with a positive center (*i.e.* the surface Ti cations), as observed for instance in homogeneous complexes when the phenolate is interacting with a Cu^{2+} [24].

The presence of a doublet for the ν(CO) mode could be indicative of the formation of monodentate phenates on structurally slightly different TiO pairs (*e.g.* located on different faces of the TiO_2 nanocrystals) [25,26] or can be explained by the formation of both monodentate and bidentate species, as already suggested for phenol adsorption on alumina [27].

In the 3800–3100 cm^{-1} region, typical of the ν(OH) manifestations (inset of Fig. 3a), the relatively narrow band at 3617 cm^{-1} is due to the stretching mode of OH groups formed by dissociative chemisorption of phenol and likely interacting with the adjacent adsorbed phenolate since their stretching frequency is lower with respect to isolated hydroxyls on clean anatase surfaces [26,28,29]. The broader absorption centered at 3490 cm^{-1} is due to OH groups experiencing stronger hydrogen bonding. Upon increasing the coverage, we can notice the progressive growth of a very broad absorption at *ca.* 3300 cm^{-1}, which becomes more evident when the phenol coverage is increased and arises from strongly hydrogen bonded phenol molecules. This band, which finds its analogue in the spectrum of solid phenol (Fig. 2), is indicative of multilayer formation on top of the first layer of chemisorbed species. The growth of this broad band is accompanied by additional manifestations, typical of the condensed phase (Fig. 3a), which appear at 1605, 1368 and 1221 cm^{-1}, suggesting that, once the surface is saturated by the phenolate and OH groups, undissociated phenol is adsorbed forming a multilayer. This phenol excess can be easily removed by outgassing at room temperature, while the dissociated phase is irreversibly adsorbed.

In order to investigate the role of adsorbed water in the photodegradation process, we investigated the effect of increasing water pressures on pre-adsorbed phenol. Initially a sub-monolayer

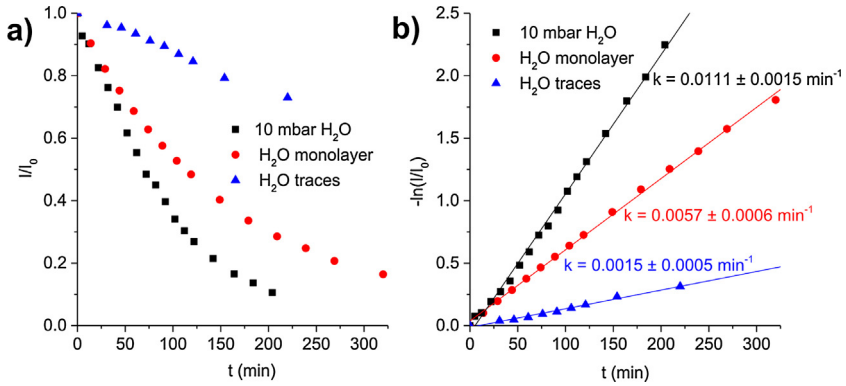

Fig. 5. a) Time evolution under UV–vis irradiation of the integrated absorbance, normalized by the absorbance before irradiation, for the phenol ν(C—O) band centered at ca. 1265 cm^{-1} in presence of different amounts of co-adsorbed water: traces of molecular water (blue triangles), surface water monolayer (red circles), 10 mbar of H_2O in equilibrium in the gas phase (black squares). The corresponding IR spectra are reported in Fig. 4. b) First order kinetic plot obtained from the data reported in part a). (For interpretation of the references to color in this figure legend, the reader is referred to the web version of this article.)

dose of phenol was adsorbed on the activated P25 surface (blue spectrum in Fig. 3b), then increasing water doses (0.1, 0.5, 1, 3, 6 and 10 mbar equilibrium pressure, black spectra in Fig. 3b) were sent, giving rise to the water bending mode, which initially appears at 1620 cm^{-1} (FWHM *ca.* 25 cm^{-1}), confirming the presence of water coordinated to Ti^{4+} centers [12]. Upon increasing the water equilibrium pressure, the band progressively becomes broad and shifts till 1633 cm^{-1} (FWHM *ca.* 80 cm^{-1}), gradually approaching to the value typical for liquid water and indicating the formation of a water multilayer [12]. In parallel a broad absorption, arising from hydrogen bonding between water molecules and dissociated phenol and between water molecules in the growing multilayer, raises in the 3600–3000 cm^{-1} spectral region.

Concerning the effect of water on the phenol vibrational modes, we can notice that water induces only a small redshift of the band at 1590 cm^{-1}, but has a strong effect on the doublet of bands previously centered at 1490 cm^{-1} and 1480 cm^{-1}, which is now substituted by a signal centered at 1484 $cm^{-1}$with a shoulder at 1494 cm^{-1} when a water multilayer is present. Also the ν(CO) doublet at 1289 and 1273 cm^{-1} is considerably modified and becomes broad and finally centered at 1266 cm^{-1} with a shoulder at 1278 cm^{-1}. At high water pressures the spectra look very similar to those obtained adsorbing phenol from a water solution [20] and the appearance of a weak absorption around 1370 cm^{-1}, related to the δ(OH) bending, confirms that some phenate species are converted back to molecular phenol.

3.2. *FTIR study of phenol photodegradation under* in situ *UV–vis irradiation*

On the basis of the results obtained studying the mechanism of phenol adsorption discussed in the previous section, to investigate the surface processes occurring during phenol photodegradation, we prepared an initial model surface state by adsorbing about 0.2 monolayer of phenol on activated P25 and, then, we varied the amount of co-adsorbed molecular water. Experiments performed in vacuum highlighted that the photodegradation is hindered in absence of oxygen, even if co-adsorbed water is present (see Fig. S2 in the supplementary data), therefore during irradiation the samples were kept in contact with 500 mbar of a 20% O_2–80% N_2 mixture. The observation that, even for long irradiation times, in absence of oxygen no substantial decrease of the phenol signals is noticeable (see Fig. S2) proves that the decrease of the phenol signals in presence of oxygen is associated to a photocatalytic process and not to thermal desorption, confirming that the sample heating by the UV–vis irradiation is negligible.

Fig. 4a shows the phenol photodegradation spectra at increasing irradiation times (up to 220 min) when only traces of molecular water are present on the oxide surface, as testified by the presence of a weak band centered at 1620 cm^{-1}, ascribed to the bending mode of water coordinated to Ti^{4+} sites. As discussed in the previous section, the spectra are dominated by the presence of phenate species which absorb at 1590, 1490, 1481, 1286, 1272, 1163 and 1151 cm^{-1}. In these hydration conditions the photodegradation reaction appears very slow and no significant signals related to the products are visible even after more than 200 min of UV–vis irradiation.

The situation is completely different when a full monolayer of co-adsorbed water is present on the P25 surface (Fig. 4b). The peak of the water bending mode is now intense and centered at 1625 cm^{-1} and the phenol vibrational modes are perturbed by the presence of water as described in the previous Section. At increasing irradiation times, we can see that the main phenol bands, *i.e.* the ν(C—H) at 3070 cm^{-1}, the ν(C=C) at 1590 and 1484 cm^{-1} and the ν(C—O) at 1266 cm^{-1}, progressively disappear, while new signals related to the products raise. In the meantime, the ν(O—H) band of hydrogen bonded water in the 3600–3100 cm^{-1} spectral region and

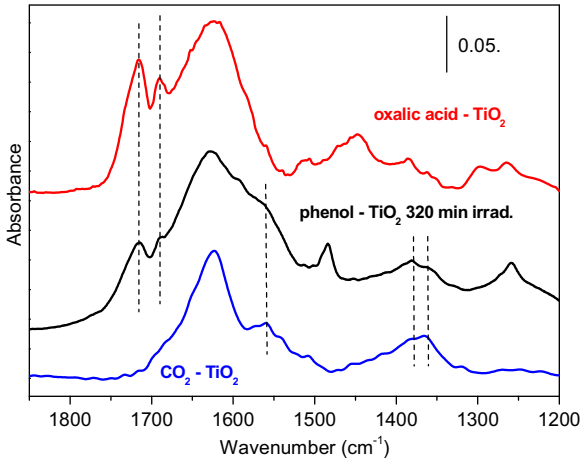

Fig. 6. FTIR spectrum of phenol photodegradation with a monolayer of co-adsorbed water on TiO_2 P25 after 320 min of UV–vis irradiation (black curve) compared with the FTIR spectra of oxalic acid (red curve) and CO_2 (blue curve) adsorbed on P25 in the same surface hydration conditions. (For interpretation of the references to colour in this figure legend, the reader is referred to the web version of this article.)

the signal associated to the water bending mode experience a small increase. The main signals of the products, which are progressively formed, are centered at 1715, 1690, 1560 and 1380–1360 cm^{-1}. The peaks around 1700 cm^{-1} can be ascribed to ν(C=O) stretching modes of carboxylic acids [8], while the bands around 1560 and 1380–1360 cm^{-1} are associated with the formation of surface carbonates [30,31]. These findings are in agreement with the most commonly proposed mechanisms of phenol photodegradation which suggest that phenol is initially converted to catechol, p-benzoquinone and hydroquinone, then to short chain acids and finally to CO_2 and water [14]. While in the ordinary experimental procedure these species are found in the solution surrounding the illuminated sample, in our experiment they are observed as adsorbed species. It is worth commenting that the presence of small quantities of catechol and hydroquinone on the P25 surface as reaction intermediates during the photodegradation process cannot be excluded since the main IR signals of these compounds fall in the same spectral region of the most intense phenol bands and hence their identification can be troublesome.

The photodegradation reaction appears even more efficient when pre-adsorbed phenol is contacted with an H_2O equilibrium pressure of 10 mbar (Fig. 4c). In these conditions a multilayer of adsorbed water is present on the TiO_2 surface (see the scheme in the right part of Fig. 4c) as demonstrated by the broad and strong band centered at 1633 cm^{-1}, related to the water bending mode, and by the presence of the roto-vibrational profile of water in the gas phase. The results obtained in these surface conditions, being more directly comparable to the processes that are occurring when the oxide surface is immersed in solution, demonstrate that the gap between surface science studies and conventional experiments in solution can be closed by appropriate dosages of water to form multilayer structures.

A quantitative analysis of the phenol photodegradation kinetics as a function of the amount of co-adsorbed water can be performed by considering the time evolution of the main phenol signals. Fig. 5a reports the time evolution under UV–vis irradiation of the integrated absorbance, normalized by the absorbance before irradiation, for the phenol ν(C—O) band for the spectra reported in Fig. 4. Considering the corresponding kinetic plot reported in Fig. 5b, we can infer that the overall reaction occurs following an apparent pseudo-first kinetic order with respect to phenol, as reported in the literature [14,32]. The pseudo-first order rate constants are strongly dependent on the surface hydration conditions and increase from 0.0015 ± 0.0005 min^{-1} for the sample containing only traces of molecular water, to 0.0057 ± 0.0006 min^{-1}, when a full monolayer of water ìs co-adsorbed with phenol, and finally to 0.0111 ± 0.0015 min^{-1} when 10 mbar of H_2O in equilibrium in the gas phase are present. Hence the rate constant increases of one order of magnitude moving from a nearly dehydrated surface to a surface with a multilayer of adsorbed water. This result demonstrates beyond any doubt that adsorbed water is an essential ingredient in the photodegradation process.

To further confirm the assignment proposed above for the reaction products, we adsorbed CO_2 and oxalic acid on the surface of P25 in the same hydration conditions used for phenol photodegradation with a full monolayer of co-adsorbed water (as testified by the similar position and intensity of the H_2O bending mode at 1625 cm^{-1} in the spectra in Fig. 6). The bands at 1715 and 1690 cm^{-1} appear to be completely compatible with the ν(C=O) of a chemisorbed oxalate as discussed also in previous studies [33]. The preferential formation of oxalic acid with respect to other short chain carboxylic acids is confirmed by the absence of the ν(C—H) stretching modes in the 3000–2800 cm^{-1} spectral region for the spectra acquired during the photodegradation. Indeed, these signals would be expected for the majority of short chain acids which has been also reported as intermediates in the phenol photodegradation (*e.g.* propionic acid, acetic acid, formic acid) [14,34].

The final mineralization of the organic compounds leads to the formation of H_2O and CO_2 which is adsorbed on the P25 surface as carbonates. These species give rise to the ν(CO) asymmetric stretching bands at 1560 and 1380–1360 cm^{-1} [30,31] and can be clearly recognized comparing the phenol spectra during the photodegradation with the spectra of CO_2 adsorbed on TiO_2 P25 (blue curve in Fig. 6).

4. Conclusions

A transmission FTIR set-up was developed to investigate photocatalytic reactions under *in situ* UV–vis illumination allowing to operate in controlled atmosphere and overcoming some of the limitations usually experienced by ATR-FTIR set-ups. This system was successfully employed to study the evolution of the surface species during the photodegradation of phenol adsorbed in controlled atmosphere on the TiO_2 P25 surface in presence of a well-defined amount of water and oxygen.

Phenol dosage from the gas phase on activated TiO_2 P25 resulted in dissociative adsorption for coverages below the monolayer and in the formation of a multilayer of undissociated phenol beyond this limit. When increasing water pressures are dosed on the pre-adsorbed phenol, the spectra become very similar to those obtained adsorbing phenol from a water solution and the appearance of a band at about 1370 cm^{-1}, related to the δ(OH) bending, confirms that some phenate species are converted back to molecular phenol.

To achieve an efficient photodegradation the presence of oxygen resulted to be crucial, therefore the photodegradation experiments were performed preparing a model surface by adsorbing about 0.2 monolayer of phenol on activated P25 and then co-adsorbing different amounts of water in presence of a 20% O_2–80% N_2 mixture. During UV–vis irradiation the main phenol signals, *i.e.* the ν(C—H) at 3070 cm^{-1}, the ν(C=C) at 1590 and 1484 cm^{-1} and the ν(C—O) at 1266 cm^{-1}, progressively decrease, while new bands, centered at 1715, 1690, 1560 and 1380–1360 cm^{-1}, appear. These signals suggest the formation of adsorbed carboxylates (mainly oxalates) and then the final conversion to H_2O and CO_2 which remains adsorbed on the TiO_2 P25 surface as carbonates. Also the presence of small quantities of catechol and hydroquinone, often reported in the reaction mechanisms discussed in the literature [14], as reaction intermediates cannot be excluded since the main IR signals of these compounds fall in the same spectral region of the most intense phenol bands.

A quantitative analysis of the phenol photodegradation kinetics as a function of the amount of co-adsorbed water was performed by considering the time evolution of the main phenol signals. The pseudo-first order rate constants resulted to be strongly dependent on the surface hydration conditions and increase of one order of magnitude moving from a nearly dehydrated surface to a surface in equilibrium with 10 mbar of H_2O in the gas phase. The latter surface conditions lead to the presence of a multilayer of liquid-like adsorbed water and can therefore be considered representative of the processes occurring at the oxide surface when TiO_2 is immersed in solution like in most applications.

Taken as a whole, these results demonstrate that: i) the method adopted in this study allows to investigate with unprecedented precision the evolution of the species adsorbed or in close contact with the surface of TiO_2 during irradiation; ii) co-adsorbed water plays a key role to promote the photocatalytic phenol degradation; iii) the gap between surface science studies on one side and studies carried out in solution on the other side can be closed by varying in a controlled way the water coverage from sub-monolayer to multilayer conditions.

Acknowledgement

The financial support of the FP7 European project SETNanoMetro—Shape-engineered TiO_2 nanoparticles for metrology of functional properties: setting design rules from material synthesis to nanostructured devices (Project number 604577) is gratefully acknowledged.

Appendix A. Supplementary data

Supplementary data associated with this article can be found, in the online version, at http://dx.doi.org/10.1016/j.apcatb.2016.05.029.

References

[1] M.R. Hoffmann, S.T. Martin, W.Y. Choi, D.W. Bahnemann, Chem. Rev. 95 (1995) 69–96.
[2] A. Fujishima, X.T. Zhang, D.A. Tryk, Surf. Sci. Rep. 63 (2008) 515–582.
[3] M.A. Henderson, Surf. Sci. Rep. 66 (2011) 185–297.
[4] N. Serpone, A.V. Emeline, J. Phys. Chem. Lett. 3 (2012) 673–677.
[5] A. Yamakata, T. Ishibashi, H. Onishi, J. Phys. Chem. B 105 (2001) 7258–7262.
[6] S. Shen, X.L. Wang, T. Chen, Z.C. Feng, C. Li, J. Phys. Chem. C 118 (2014) 12661–12668.
[7] P.Z. Araujo, C.B. Mendive, L.A.G. Rodenas, P.J. Morando, A.E. Regazzoni, M.A. Blesa, D. Bahnemann, Colloid Surf. A-Physicochem. Eng. Asp. 265 (2005) 73–80.
[8] I. Dolamic, T. Burgi, J. Catal. 248 (2007) 268–276.
[9] D.M. Savory, D.S. Warren, A.J. McQuillan, J. Phys. Chem. C 115 (2011) 902–907.
[10] C.B. Mendive, T. Bredow, J. Schneider, M. Blesa, D. Bahnemann, J. Catal. 322 (2015) 60–72.
[11] A. Atifi, K. Czarnecki, H. Mountacer, M.D. Ryan, Environ. Sci. Technol. 47 (2013) 8650–8657.
[12] M. Takeuchi, G. Martra, S. Coluccia, M. Anpo, J. Near Infrared Spectrosc. 17 (2009) 373–384.
[13] A. Sobczynski, L. Duczmal, W. Zmudzinski, J. Mol. Catal. A-Chem. 213 (2004) 225–230.
[14] E. Grabowska, J. Reszczynska, A. Zaleska, Water Res. 46 (2012) 5453–5471.
[15] L. Mino, G. Spoto, S. Bordiga, A. Zecchina, J. Phys. Chem. C 117 (2013) 11186–11196.
[16] S.M. Jain, J.J. Biedrzycki, V. Maurino, A. Zecchina, L. Mino, G. Spoto, J. Mater. Chem. A 2 (2014) 12247–12254.
[17] M. El-Roz, M. Kus, P. Cool, F. Thibault-Starzyk, J. Phys. Chem. C 116 (2012) 13252–13263.
[18] M. El-Roz, P. Bazin, M. Daturi, F. Thibault-Starzyk, Phys. Chem. Chem. Phys. 17 (2015) 11277–11283.
[19] J.C. Evans, Spectrochim. Acta 16 (1960) 1382–1392.
[20] L. Palmisano, M. Schiavello, A. Sclafani, G. Martra, E. Borello, S. Coluccia, Appl. Catal. B-Environ. 3 (1994) 117–132.
[21] D. Michalska, W. Zierkiewicz, D.C. Bienko, W. Wojciechowski, T. Zeegers-Huyskens, J. Phys. Chem. A 105 (2001) 8734–8739.
[22] A. Zecchina, G. Spoto, S. Bordiga, Handbook of Vibrational Spectroscopy, in: J.M. Chalmers, P.R. Griffiths (Eds.), John Wiley & Sons Ltd., Chichester, 2002.
[23] M. Miyazaki, A. Kawanishi, I. Nielsen, I. Alata, S. Ishiuchi, C. Dedonder, C. Jouvet, M. Fujii, J. Phys. Chem. A 117 (2013) 1522–1530.
[24] P. Milko, J. Roithova, N. Tsierkezos, D. Schroder, J. Am. Chem. Soc. 130 (2008) 7186–7187.
[25] L. Mino, A.M. Ferrari, V. Lacivita, G. Spoto, S. Bordiga, A. Zecchina, J. Phys. Chem. C 115 (2011) 7694–7700.
[26] L. Mino, G. Spoto, S. Bordiga, A. Zecchina, J. Phys. Chem. C 116 (2012) 17008–17018.
[27] A. Popov, E. Kondratieva, J.P. Gilson, L. Mariey, A. Travert, F. Mauge, Catal. Today 172 (2011) 132–135.
[28] C. Deiana, E. Fois, S. Coluccia, G. Martra, J. Phys. Chem. C 114 (2010) 21531–21538.
[29] S. Higashimoto, K. Okada, M. Azuma, H. Ohue, T. Terai, Y. Sakata, RSC Adv. 2 (2012) 669–676.
[30] G. Martra, Appl. Catal. A-Gen. 200 (2000) 275–285.
[31] L. Mino, G. Spoto, A.M. Ferrari, J. Phys. Chem. C 118 (2014) 25016–25026.
[32] D. Dumitriu, A.R. Bally, C. Ballif, P. Hones, P.E. Schmid, R. Sanjines, F. Levy, V.I. Parvulescu, Appl. Catal. B-Environ. 25 (2000) 83–92.
[33] C.B. Mendive, D.W. Bahnemann, M.A. Blesa, Catal. Today 101 (2005) 237–244.
[34] A. Turki, C. Guillard, F. Dappozze, Z. Ksibi, G. Berhault, H. Kochkar, Appl. Catal. B-Environ. 163 (2015) 404–414.